

A fast modal wave-front sensor

Erez N. Ribak

Department of Physics, Technion – Israel Institute of Technology, Haifa 32000, Israel

Steven M. Ebstein

Lexitek, Inc., 14 Mica Lane #6, Wellesley, MA 02481, USA

Abstract: We describe an instantaneous modal wave-front sensor. The sensor uses a Shack-Hartmann lenslet array to encode the wave-front distortion. A novel parallel electro-optic processor continuously converts the spot pattern to wave-front modes, e.g. Zernike polynomials, without a separate reconstructor. Using readily available components, the sensor can achieve MHz bandwidths for twenty modes. The bandwidth, sensitivity, and number of bits can vary for each mode to match the sensor to the disturbance in an optimal fashion. The proposed sensor has immediate application to beam control and turbulence sensing applications that require wide bandwidths. The measured wave-front modes can also be those of an adaptive optics system, directly providing control signals for the actuators of a deformable mirror. A similar electronic reconstructor mode is also described.

©2001 Optical Society of America

OCIS codes: 010.1080 Adaptive optics; 200.0200 Optical computing

References and links

1. S. M. Ebstein and E. N. Ribak, Proposal to DOD, SBIR AF97-105, 1997.
2. C. Schwartz, E. N. Ribak, and G. Baum: "Implications of fractal structure of turbulence degraded wave fronts" *J. Opt. Soc. A* **11**, 444-51 (1994).
3. M. A. A. Neil, M. J. Booth and T. Wilson, "New modal wave-front sensor: a theoretical analysis" *J. Opt. Soc. A* **17**, 1098-107 (2000).
4. A. Wirth, J. Feinleib, L. E. Schmutz, D. H. Rapkine, R. F. Dillon, and J. J. Hizny, "Optical wavefront sensing system" US Patent 4725138 (1988).
5. C. Pappalolios, P. Nisenson, and S. Ebstein, "Speckle Imaging with the PAPA Detector" *Applied Optics* **24**, 285-9 (1985).
6. W. J. Wild, "Innovative wavefront estimators for zonal adaptive optics systems" Ch. 6 in *Adaptive Optics Engineering Handbook*, Ed. R. K. Tyson (Marcel Dekker, New York, 2000).

Wave-front sensors usually fall into one of two types: gradient sensors and curvature sensors. Gradient sensors rely on a lenslet array (Hartmann-Shack) or shearing interferometers. Curvature sensors have fewer optical requirements: they need to measure the intensity in front and behind the focus of the optical system. Hartmann-Shack sensors require only one fast, sensitive camera, whereas shearing interferometers and curvature sensors require two cameras, or a complex optical design to multiplex two images on the same camera. After detection (by a sensitive CCD camera or an array of single photon detectors), the detector signal is digitized. Once the gradients or curvatures are measured, they need to be integrated numerically once or twice to describe the wave-front in some manner, such as by Zernike coefficients. This is usually done by multiplying the input vector by some matrix to produce a vector output of coefficients. In adaptive optics, the output coefficients are actually control signals for the mirror actuators. These computations require that a fast, dedicated processor be included as part of the sensor. The processor usually limits the sensor bandwidth and complicates the system.

We propose to circumvent most of this process by using opto-electronic processing to directly calculate and then detect a chosen representation of the wave-front, in either an analog or digital form. The signal modes can be chosen at will, such as Zernike or Karhunen-Loeve polynomials, voltages for the actuators in a deformable mirror¹ or atmospheric fractal components². Recently a similar system was constructed to procure the modes of coherent wave-fronts, such as those arriving from a laser, by utilizing a holographic processor³. However, what we suggest here refers also to wave-fronts emanating from incoherent sources.

We point out that optical processing is not a novel idea for wavefront sensing. One example is a method that was devised to measure the centroids of Hartmann-Shack spots⁴. Our approach, however, introduces the concept of modal optical processing using Hartmann-Shack spots to the published literature.

We start with a lenslet array, such as in every Hartmann-Shack sensor, producing (in the case of a flat wave-front) a regular grid of M foci spots. The wave-front aberrations are encoded into the pattern of the foci as their shift from their central positions, proportional to the local gradient of the wave-front (G_i in Figure 1a). This pattern is detected and amplified, turning it into an incoherent image of the focal spots (H_i). Then it is multiplexed optically into N parallel copies of the spot pattern, a copy D_j for each mode to be detected. Each such copy of the pattern is then multiplied optically by an appropriate mask, M_j , and the result gathered into a single detector, the signal of which representing the mode (P_j). This is an optical realization of vector-matrix multiplication: the image is copied many times over, once for each row of the matrix, then multiplied by this row, and finally added up by a single detector.

The processor is a novel parallel optical computer modeled on the PAPA photon-tagging camera⁵. A lenslet array, placed in a distorted beam forms an array of M Hartmann spots, which are focussed on the input of an image intensifier (Figure 1b). A collimator and a lens array make N multiple images of the Hartmann spot array. The images fall on an array of $N \times M$ submasks. N discrete photodetectors sense the light that passes through the partially transmitting N masks. There are three possible outputs: analog, analog converted electronically to digital, and digital like the PAPA. Here, each mode is split into a few binary bits, and detected in parallel masks, detectors, and discriminators.

This process can be described as an array of multiplying masks that transfers the Hartmann pattern of spots to a set of parallel outputs that are the coefficients of the required modes. We shall use Zernike polynomials as example modes throughout this paper. Each mode has a unique pattern corresponding to a shift of the M Hartmann spots, and this unique pattern is measured by one of the N masks. In what follows, we assume that one channel is clear and measures the integrated intensity across the beam. All measurements are scaled by that integrated intensity. Because of the averaging effect of the plurality of foci spots, this channel might not be necessary: the scaling might be done with the average of all masks.

Scintillation of the incoming beam will add a spatially varying weight to the output of the sensor. The weighting is proportional to the intensity of the Hartmann spots multiplied by the mask, which is related to the light amplitude across the pupil. As long as the scintillation is not so severe as to exceed the dynamic range of the intensifier, the sensor output should be a linear function of the intensity.

As an example, consider a tip (x -tilt) term, where all Hartmann foci will shift horizontally in an amount relative to the wave-front slope. The average location of the set of spots will be measured by a corresponding set of masks. These masks are matched to the corresponding focal positions of the Hartmann spots. In the example shown in Figure 2, the mask at the top left is used to measure the tip. The mask has vertical stripes whose edges fall in the center of each Hartmann spot subfield. A comparator set to one-half the integrated intensity determines how much are the spots to the left or the right of the center, as averaged over all of the wave-front. Similar information is gained from the y -tilt mask next to it.

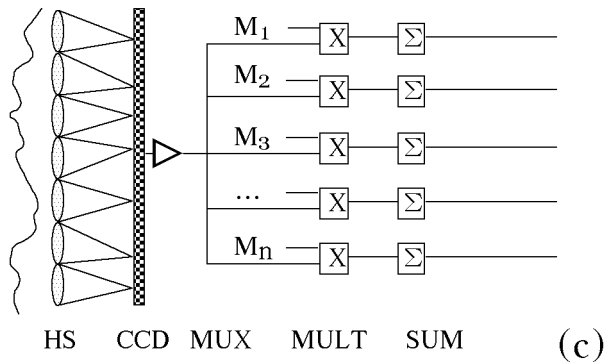
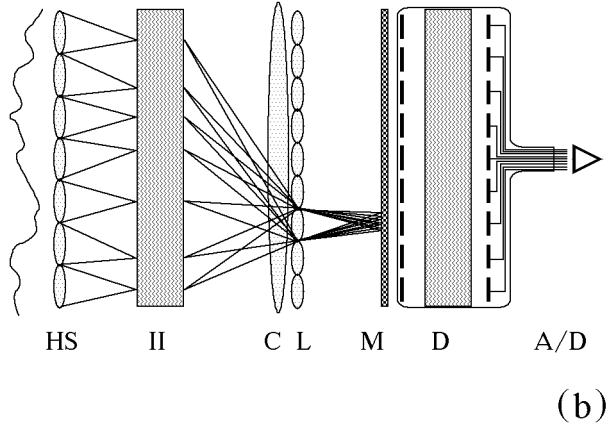
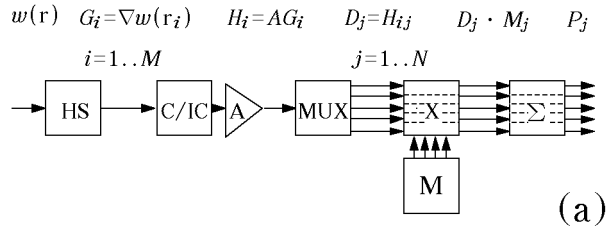


Figure 1: Modal wave-front sensor: (a) schematic model, (b) optical and (c) electronic realizations. HS Hartmann Shack lenslet array; C/IC coherent to incoherent converter; A amplifier; MUX multiplexer; M mask array; X, MULT multiplier; Σ , SUM integrator; II image intensifier; C collimator; L lens array; D detector array; A/D analog to digital converter.

The next mask at the top row encodes the focus term. With defocus, the Hartmann foci shift radially inside or outside according to the sign of the coefficient. Hence they are multiplied by masks made of tangential wedges that encode the radial position. The masks reduce the intensity of the spots that are shifted radially inward and pass more of the spots that shifted outward, providing the average defocus across the wave-front.

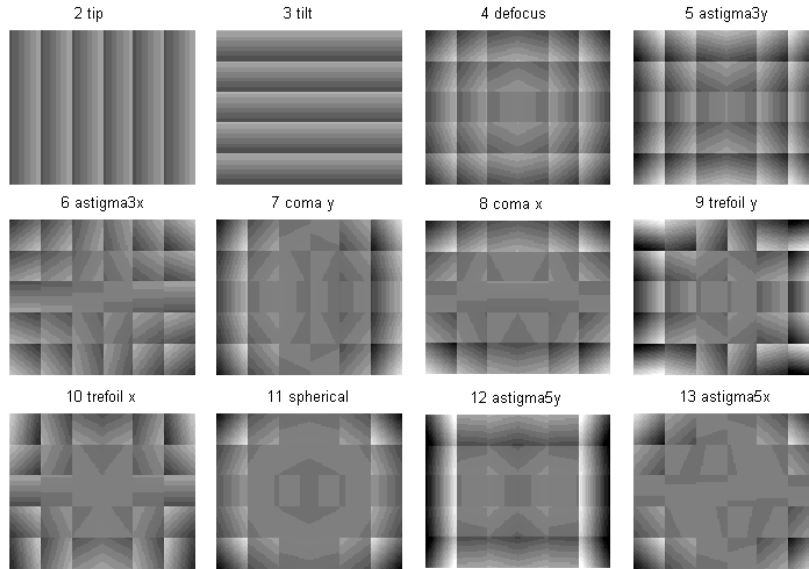


Figure 2: The first twelve Zernike masks. Light from a copy of the Hartmann pattern with thirty spots impinges on each mask and the signal integrated by a single mode detector.

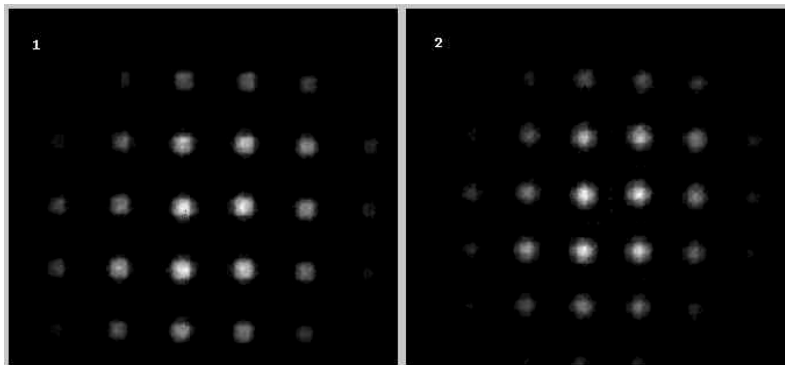


Figure 3: Two Hartmann patterns from a laser beam, differing mainly in focus and tilt.

We have applied this set of masks to two patterns of Hartmann spots obtained from a laser (Figure 3). For the two patterns we moved the sensor equally in opposite directions, introducing mostly a tip and focus error. The results are summarized in Table 1.

Table 1: Zernike Coefficients for the masks shown in Figure 2 and the two patterns shown in Figure 3.

Mode #	2	3	4	5	6	7	8	9	10	11	12	13
Name	Tip	Tilt	Def	Astig 3	Astig 3	Coma y	Coma x	Tref y	Tref x	Spher	Astig 5	Astig 5
# 1	-0.141	-0.413	-0.358	-0.067	0.002	-0.098	0.164	-0.008	-0.071	-0.215	-0.226	-0.042
# 2	-0.092	0.405	0.358	0.082	-0.097	-0.026	-0.207	-0.101	0.001	0.181	0.192	0.039

In the example above, we assumed that the spots are small compared to the mask size. Another option is to have binary masks and large Hartmann spots, either due to intentional defocusing or to a large $f/\#$ of either lenslet array. Consider a pure Zernike mode where all of the spots move uniformly across their respective submask boundaries. As each spot translates

across a sharp boundary, the light increases linearly from zero to full strength. The integrated signal, through all the submasks, can then be either analogue or digital.

In the mode most similar to the PAPA camera, the spots are small and the masks binary. This should give a single bit, according to whether the spots are blocked by the submasks or not. The next bits are provided by finer binary masks, parallel to the former ones at half the spacing. A comparator decides whether that bit is above or below the mean signal.

The design of the submasks for Zernike modes is simple: The basic notion is that the submask gradient is oriented parallel to the average gradient across each Hartmann lenslet for a particular Zernike mode. The slope is linear with the expected gradient of the wave front at that specific submask. At the middle position, half of the light passes through the submask. If the spots are large, the mask slope is not linear any more: it is the Wiener deconvolution of the spot shape from the linear output signal, incorporating a noise model.

An intriguing notion is the possibility of directly calculating control signals for deformable mirror actuators. A possible approach is pictured schematically in Figure 4 where a set of actuators is assumed arranged coincident with the 3x3 Hartmann lenslets. This approach integrates the wave-front tilts from a reference point to each actuator. The upper left actuator defines the reference point (0,0). The mask labeled 'actuator 1,0' integrates the tilt from the upper left to the next actuator to the right. All other tilts (Hartmann spots) are blocked. The 'actuator 2,0' mask integrates the tilt to the second actuator to the right of the reference. The 'actuator 1,1' mask integrates the tilt to the actuator one right and one down. Note that there are two paths to this point: right then down and down then right. The mask passes light from the four spots in the upper left corner, which encompass both of those paths. The basic notion is that the mask boundaries are normal to the vector from each spot to the target actuator and only spots within the rectangle defined by the reference and the target actuator are passed. This approach does not treat all spots equally – those closest to the reference are preferred. In a simpler zonal approach, each actuator receives signals from its nearest neighbors (such as the focus mask in Figure 2) equal to its influence function, while global tip and tilt are measured as before and transmitted to a separate mirror.

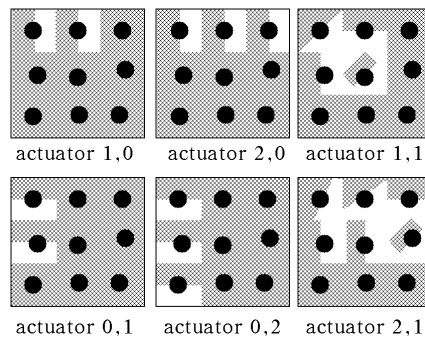


Figure 4: Integrating the signals from the central element (0,0) at the top left. Each actuator signal amounts to integration from the center to its position along a few shorter paths.

More research is needed before one could conclude that direct real-time control implemented similar to what is shown in Figure 4 is useful. We have not considered the noise performance of such a system and how systematic effects such as imperfections in the components or construction or biases in the control outputs would affect the performance.

How are the masks calculated? Since we know in advance the Hartmann-Shack pattern and the influence functions of the actuator, we can calculate the pseudoinverse response matrix⁶. Each row in the matrix, representing an actuator, has $2M$ elements on it, corresponding to the M spots (each supplying two orthogonal components). The corresponding mask element is normal to the direction given by these two components, and its strength is their vectorial sum.

The principal advantage of the sensor is its speed of operation. Each wave-front mode is measured, in parallel, by a photosensor that integrates over the entire pupil. The read out rate can be different for different modes. The bandwidth of the sensor is limited by the speed of the various components. If the final photosensors are discrete or an array of photomultipliers or avalanche photodiodes, they impose a limit of $10^8 - 10^9$ Hz. The image intensifier at the front of the detector is the main limit: fast phosphors have decay times of $\sim 10^{-7}$ s. Faster, but less efficient, phosphors are also possible. If the light intensity is even higher, there is no need for the image intensifier (Figure 1b), and a simple scatterer can replace the incoherent-to-coherent converter. Ground glass and directional holographic devices are such scatterers.

It is instructive to consider the noise performance of the detector. The example we consider uses masks like in Figure 2 to sense the modes. We consider a case where scintillation is not present so each of the M spots produces K photoelectrons, on average, at the intensifier. We assume that the detector is perfectly aligned and the mean number of photons is known. This allows the zero signal point (perfectly flat wavefront) to be perfectly estimated. We will consider the measurement variance of a single mode about that point, so it is equivalent to consider a grayscale mask or a binary mask with the spots nominally centered on the mask boundaries. Either mask yields $K/2$ signal events, on average, per spot, with normalized Poisson variance of $2/K$. If the intensifier gain is sufficient, only the statistics of the intensifier photodetection and its excess noise due to amplification matter, i.e., the downstream measurement noise is irrelevant. We assume the excess noise factor is 1.33 (a minimum). Since each Hartmann-Shack spot is independent, the variance scales as $1/M$ and the net variance is $(2 \times 1.33/MK)$.

The concept is not limited to the light input being structured by a Hartmann array. Instead, curvature signals before and after the focus could be provided, or fringes from two shearing interferometers could serve as input. For each one of these options, a different set of masks would be required. However, it seems that because of the discrete nature of the Hartmann spots, they are best matched to the optical processor. Notice that one usually tries to have as few spots as possible so as to increase the photon content of each. Here this limitation does not exist, and the spots can be made as dense as the optical transfer function will allow.

A somewhat slower version of the device can be realized electronically. In this version (Figure 1c), a CCD detects the Hartmann spots. The signal is digitized electronically and multiplexed into the number of channels required. Stored masks, produced in the same manner as the optical masks, are multiplied on the fly with the CCD pixels as they come out of the camera (this is a standard feature in commercial frame grabbers). The integrated signal is received as soon as the frame is read out. This operational mode removes the need for digital centroiding of the individual spots, and later the multiplication of the centroid signals by the response mask. However, it does include CCD pixels that can be avoided when reading only the Hartmann spots, somewhat slowing the read out.

The main advantage of the modal wave-front sensor is its speed. On the other hand, it has some limitations, all rising from it being an optical processor. Such devices tend to be of a limited dynamic range. In the first place, optical design makes it difficult to multiplex the Hartmann pattern more than approximately twenty times. This is then the number of modes detectable with this device. The efficiency is limited by the detectors and masks: image intensifiers have at most a quantum efficiency of 20%, and in the electronic version the CCD has a few read-out electrons per pixel. The masks block on the average 50% of the light. Another disadvantage of the device is its inflexibility: changing the Hartmann pattern requires a new set of masks. If the masks are gradual (gray levels), they have to be prepared separately. A spatial light modulator with a large number of addressable pixels could possibly be useful for fabricating a flexible version of this sensor.